Pergamon

Int. J. Solids Structures Vol. 32, No. 16, pp. 2345–2367, 1995

0020-7683/95 $9.50 + .00

0020-7683(94)00229-0

A REFINED HYBRID PLATE THEORY FOR COMPOSITE LAMINATES WITH PIEZOELECTRIC LAMINAE

J. A. MITCHELL and J. N. REDDY
Department of Mechanical Engineering, Texas A & M University, College Station, TX 77843-3123, U.S.A.

(*Received* 25 *March* 1994; *in revised form* 8 *September* 1994)

Abstract—In this paper, a refined theory of laminated composite plates with piezoelectric laminae is developed. The equations of motion of the theory are developed using an energy principle. This formulation is based on linear piezoelectricity, and includes the coupling between mechanical deformations and the charge equations of electrostatics. The theory developed herein is hybrid in the sense that an equivalent single-layer theory is used for the mechanical displacement field, whereas the potential function for piezoelectric laminae is modeled using a layerwise discretization in the thickness direction. For the equivalent single layer, the third-order shear deformation theory of Reddy is used. This hybrid feature is good in that it demonstrates a way in which multilayered smart skin piezoelectric structures may be analysed to accommodate multiple voltage inputs and/or sensor outputs.

1. INTRODUCTION

The study of embedded or surface-mounted piezoelectric materials in structures has received considerable attention in recent years. One reason for this is that it may be possible to create certain types of structures and systems capable of adapting to or correcting for changing operating conditions. The advantage of incorporating these special types of material into the structure is that the sensing and actuating mechanism becomes part of the structure by sensing and actuating strains directly. These types of mechanisms are referred to as strain sensing and actuating (SSA). This advantage is especially apparent for structures that are deployed in space. Generally, space-borne structures are very flexible because they are not designed for operations in which the force of gravity is present. In addition, they are characterized as having very low levels of damping. Thus, transient vibrations endure for longer periods of time than is acceptable and operations may be interrupted. Proof-mass actuators, thrusters, and piezoelectric materials as described here are possible means of controlling the vibrations. Of course, there may also be many other good methods that have not as yet been thought of. However, generally speaking, most actuator systems other than the strain-induced type add a considerable amount of weight and possibly space to the structure, thereby changing its mechanical properties significantly.

In order to utilize the strain-sensing and actuating properties of piezoelectric materials, the interaction between the structure and the SSA material must be well understood. Mechanical models for studying the interaction of piezoelectric patches surface-mounted to beams have been developed by Crawley and de Luis (1987), Im and Atluri (1989), and Chandra and Chopra (1993). The study presented here is different from these in that we study laminated plates containing piezoelectric laminae. The SSA lamina can offer both a discrete effect similar to patches as well as a distributed effect. Lee (1990) derived a theory for laminated piezoelectric plates based on classical plate theory, where the linear piezoelectric constitutive equations were the only source of coupling between the electric field and the mechanical displacement field. Pai *et al.* (1993) have presented a geometrically non-linear plate theory for the analysis of composite plates with distributed piezoelectric laminae. However, their model does not include the charge equations of electrostatics. In constrast, Tiersten (1969) modeled single-layer piezoelectric plates, including the charge equations, but did not study laminates. Tzou and Gadre (1989) derived equations of motion

for thin laminated shells with piezoelectric layers based upon Love's first-approximation shell theory and Hamilton's principle. At that time, they did not include the charge equations in the model. Later, Tzou and Zhong (1993) derived governing equations for piezoelectric shells using first-order shear deformation theory and included the charge equations of electrostatics. From these equations, classical and first-order shear deformation plate theories were derived for single-layer piezoelectric laminae.

It is the purpose of this article to present a simple method of enhancing current plate theories to include the charge equations of electrostatics. This is accomplished by modeling the scalar potential function, from which the electric field is derived, using the layerwise approach of Reddy (1987, 1994). In this way, classical and shear deformation theories for plates can be enhanced so that a physically correct model of the piezoelectric effect can be included. The work presented here is most closely related to a paper published by Lee (1990). In contrast, the coupling between the electric field and the mechanical displacement field is modeled to include the charge equations of electrostatics.

As a final note to this introduction, we comment that for the case of plane stress as presented here, the degree of coupling between mechanical deformations and the electric field may vary from negligible to significant, depending upon the materials and loading conditions involved. However, for the case of thick plates the coupling is likely to be significant. Also, an equivalent single-layer theory (ESL) for the mechanical displacements would no longer be valid. In this case, one approach would be to model both the mechanical displacement field as well as the scalar potential using the layerwise theory of Reddy (1987). This generalized approach is discussed in a forthcoming paper by the authors [see Reddy and Mitchell (1994)]. Since the present approach combines a layerwise-type approximation with an equivalent single-layer theory (ESL), it is labeled as a refined hybrid theory.

2. FORMULATION

2.1. *Piezoelectricity*

In this paper, Hamilton's principle is applied to derive a set of approximate governing equations for laminated plates with piezoelectric laminae based on the linear theory of piezoelectricity, which in turn is based on a sequence of two approximations. First, the non-linear theory of electroelasticity is derived from the well-known conservation laws for a mechanical continuum and the conservation laws derived from Maxwells' equations [see Penfield and Haus (1967)]. In this step, a quasistatic electric field approximation is made, which allows for the electric field to be derivable from a scalar potential function. It is also assumed that the magnetic field and magnetization have negligible influence and that the electric field, polarization, and charge density are of primary concern when describing the motion and deformation of the material.

The second approximation, from whence the linear theory of piezoelectricity is derived, is that deformations are infinitesimal and that electric fields are small [see Tiersten (1981)]. In the theory, the charge equations of electrostatics are coupled to the mechanical deformations by using a modified Lagrangian function given by

$$L = \tfrac{1}{2}\rho \dot{u}_i \dot{u}_i - H(\varepsilon_{ij}, E_i), \tag{1}$$

where $H(\varepsilon_{ij}, E_i)$ is called the electric enthalpy density function, ε_{ij} are the components of the strain tensor, and E_i are the components of the electric field vector. In the present study $H(\varepsilon_{ij}, E_i)$ is taken as [see Tiersten (1969) and Reddy (1994)]

$$H(\varepsilon_{ij}, E_i) = \tfrac{1}{2}c_{ijkl}\varepsilon_{ij}\varepsilon_{kl} - e_{ijk}E_i\varepsilon_{jk} - \tfrac{1}{2}k_{ij}E_iE_j, \tag{2}$$

where c_{ijkl}, e_{ijk}, and k_{ij} are called the elastic, piezoelectric, and dielectric permittivity constants, respectively. As described above, the electric field E_i is derivable from a scalar potential function ϕ as follows:

$$E_i = -\frac{\partial \phi}{\partial x_i}. \tag{3}$$

Equations (1)–(3) describe the linear theory of piezoelectricity, which when combined with Hamilton's principle, can be used to derive a set of approximate governing equations for laminated plates. Using the above definitions, and assuming there are no body forces, the variational step leads to

$$0 = \int_0^{T_0} \int_V \{\rho \dot{u}_j \delta \dot{u}_j - \sigma_{ij} \delta \varepsilon_{ij} - D_i (\delta \phi)_{,i}\} \, \mathrm{d}V \, \mathrm{d}t + \int_0^{T_0} \int_S \{t_i \delta u_i + q \delta \phi\} \, \mathrm{d}S \, \mathrm{d}t, \tag{4}$$

where σ_{ij} and D_i are the components of the stress tensor and the electric displacement vector, respectively, derived from $H(\varepsilon_{ij}, E_i)$ as

$$D_i = -\frac{\partial H}{\partial E_i} \tag{5a}$$

and

$$\sigma_{ij} = \frac{\partial H}{\partial \varepsilon_{ij}}. \tag{5b}$$

Also note that the mechanical and electric work done by surface traction t_i and applied charge density q have been included in the functional. Here we assume that the entire surface of the dielectric is covered with electrode. Then q is the charge density that can exist in the conductor at a dielectric conductor interface. In most applications, ϕ is specified on the surface and the charge density q would be found in a postcomputation, or in sensor applications [see Lee (1990)] it may be a measured quantity.

2.2. *Displacement field*

In the third-order shear deformation theory of Reddy (1984, 1994), the displacement field is assumed to be of the form

$$u_1(x, y, z, t) = u_0(x, y, t) + g_1(z)\psi_x(x, y, t) - g_2(z)\frac{\partial w_0}{\partial x}, \tag{6a}$$

$$u_2(x, y, z, t) = v_0(x, y, t) + g_1(z)\psi_y(x, y, t) - g_2(z)\frac{\partial w_0}{\partial y}, \tag{6b}$$

$$u_3(x, y, z, t) = w_0(x, y, t), \tag{6c}$$

where (u_0, v_0, w_0) are the displacements of a point on the midplane of the laminate, and (ψ_x, ψ_y) denote the rotations of a tranverse normal at $z = 0$ about the y and $-x$ axes, respectively.

The salient feature of this particular theory is that it allows for cubic distortion of the normals to the midplane while at the same time eliminating the need for shear correction factors. This is possible because of the particular form of the functions $g_1(z)$ and $g_2(z)$, which are given as

$$g_1(z) = z - c_1 z^3, \quad g_2(z) = c_1 z^3, \quad c_1 = \frac{4}{3T^2}, \tag{7}$$

where T is the total laminate thickness and z is assumed to be measured from the laminate geometric midplane. Using these definitions, it is easy to verify that the transverse shear strains ε_4 and ε_5 are zero at the upper and lower surfaces of the plate, and vary quadratically

through the thickness. Although this particular approximation was developed for laminate plates without piezoelectric laminae, it also serves well when piezoelectric laminae are present, since contributions to the shear stress on the major surfaces due to piezoelectric laminae derive from the gradient of the potential function. Corresponding to this, a plate having piezoelectric laminae on its outer surfaces covered with a very thin electrode will not have any component of inplane electric fields on these surfaces because they are equipotential. Further, since transverse shear stresses due to piezoelectric effects result from components of the inplane electric field (this depends upon the particular form of the constitutive relationships), it follows that shear stresses on the free surfaces result due to mechanical effects only.

At this stage, the tensor notation is abandoned and the engineering notation is adopted for stresses, strains, and piezoelectric and permittivity constants. The following definitions for infinitesimal engineering strains ε_i, $i = 1, 2, \ldots, 6$ are used:

$$\varepsilon_1 = \varepsilon_{11} = \frac{\partial u_1}{\partial x_1}; \quad \varepsilon_2 = \varepsilon_{22} = \frac{\partial u_2}{\partial x_2}; \quad \varepsilon_3 = \varepsilon_{33} = \frac{\partial u_3}{\partial x_3};$$

$$\varepsilon_4 = 2\varepsilon_{23} = \frac{\partial u_2}{\partial x_3} + \frac{\partial u_3}{\partial x_2}; \quad \varepsilon_5 = 2\varepsilon_{13} = \frac{\partial u_1}{\partial x_3} + \frac{\partial u_3}{\partial x_1}; \quad \varepsilon_6 = 2\varepsilon_{12} = \frac{\partial u_1}{\partial x_2} + \frac{\partial u_2}{\partial x_1}. \tag{8}$$

The last approximation to be made in this variational formulation is for the potential function ϕ. It is convenient to model ϕ on a discrete layer approximation as follows.

$$\phi(x, y, z, t) = \sum_{j=1}^{n} f_j(z)\varphi_j(x, y, t), \tag{9}$$

where $f_j(z)$ are taken to be Lagrange interpolation functions [see Reddy (1993)]. This is equivalent to modeling the variation of ϕ through the thickness with 1-D finite elements. Non-piezoelectric laminae can be modeled by simply setting the piezoelectric constants to zero and retaining the dielectric permittivity constants if necessary. In this way it is possible to model and analyse very arbitrary applied potential loading conditions as well as more than one material type including piezoelectric.

2.3. *Constitutive relationships*

The model proposed here is useful for laminates with laminae having arbitrary orientations through the thickness. However, for derivations presented here it is assumed that the principle material coordinates coincide with the coordinates of the problem being analysed. The constitutive relationship for a material having orthorhombic *mm*2 symmetry, including piezoelectric effects, is given as follows:

$$\begin{Bmatrix} \sigma_1 \\ \sigma_2 \\ \sigma_3 \\ \sigma_4 \\ \sigma_5 \\ \sigma_6 \end{Bmatrix} = \begin{bmatrix} c_{11} & c_{12} & c_{13} & 0 & 0 & 0 \\ c_{12} & c_{22} & c_{23} & 0 & 0 & 0 \\ c_{13} & c_{23} & c_{33} & 0 & 0 & 0 \\ 0 & 0 & 0 & c_{44} & 0 & 0 \\ 0 & 0 & 0 & 0 & c_{55} & 0 \\ 0 & 0 & 0 & 0 & 0 & c_{66} \end{bmatrix} \begin{Bmatrix} \varepsilon_1 \\ \varepsilon_2 \\ \varepsilon_3 \\ \varepsilon_4 \\ \varepsilon_5 \\ \varepsilon_6 \end{Bmatrix}$$

$$+ \begin{bmatrix} 0 & 0 & e_{31} \\ 0 & 0 & e_{32} \\ 0 & 0 & e_{33} \\ 0 & e_{24} & 0 \\ e_{15} & 0 & 0 \\ 0 & 0 & 0 \end{bmatrix} \begin{Bmatrix} \frac{\partial \phi}{\partial x} \\ \frac{\partial \phi}{\partial y} \\ \frac{\partial \phi}{\partial z} \end{Bmatrix} \tag{10a}$$

$$\begin{Bmatrix} D_1 \\ D_2 \\ D_3 \end{Bmatrix} = \begin{bmatrix} 0 & 0 & 0 & 0 & e_{15} & 0 \\ 0 & 0 & 0 & e_{24} & 0 & 0 \\ e_{31} & e_{32} & e_{33} & 0 & 0 & 0 \end{bmatrix} \begin{Bmatrix} \varepsilon_1 \\ \varepsilon_2 \\ \varepsilon_3 \\ \varepsilon_4 \\ \varepsilon_5 \\ \varepsilon_6 \end{Bmatrix}$$

$$- \begin{bmatrix} k_{11} & 0 & 0 \\ 0 & k_{22} & 0 \\ 0 & 0 & k_{33} \end{bmatrix} \begin{Bmatrix} \dfrac{\partial \phi}{\partial x} \\ \dfrac{\partial \phi}{\partial y} \\ \dfrac{\partial \phi}{\partial z} \end{Bmatrix}. \quad (10b)$$

Based on this constitutive relationship, PVDF (polyvinylidene fluoride) [see Varadan *et al.* (1989) and Nix and Ward (1986)] and PZT (lead zirconate-titanate) [see Dunn and Taya (1993)] materials can be considered. In this analysis, the plane stress approximation is made, thus requiring modifications to the above constitutive relationships. By setting $\sigma_3 = 0$, the strain ε_3 is eliminated from the constitutive relationships. While the labels for the elastic, piezoelectric stress, and dielectric permittivity constants are not changed, it is assumed that they have been adjusted to accommodate the plane stress aproximation.

2.4. *Equations of motion*

In this analysis, a variational formulation is used to derive a two-dimensional theory from the fully three-dimensional theory of linear piezoelectricity. By making the approximations concerning the displacement field (u_1, u_2, u_3) and the potential function ϕ as described in previous sections, it is possible to eliminate the dependency of the primary variables (u_1, u_2, u_3, ϕ) upon the thickness coordinate z. In particular, the mechanical displacement field corresponds to an equivalent single-layer theory and the potential function approximation corresponds to a layerwise theory. To obtain the equations of motion and boundary conditions for the two-dimensional theory, approximations are substituted into eqn (4). This procedure is identical to that used for standard equivalent single-layer theories [see Reddy (1994)]. The z-dependence is integrated out by defining convenient stress and charge resultants. Boundary conditions and the Euler–Lagrange equations are then obtained from Hamilton's principle.

Proceeding as described above, eqn (4) is expanded, giving

$$\begin{aligned} 0 = & \int_0^{T_0} \int_V \rho \{ \dot{u}_1 \delta \dot{u}_1 + \dot{u}_2 \delta \dot{u}_2 + \dot{u}_3 \delta \dot{u}_3 \} \, \mathrm{d}V \, \mathrm{d}t \\ & - \int_0^{T_0} \int_V \{ \sigma_1 \delta \varepsilon_1 + \sigma_2 \delta \varepsilon_2 + \sigma_3 \delta \varepsilon_3 + 2\sigma_4 \delta \varepsilon_4 + 2\sigma_5 \delta \varepsilon_5 + 2\sigma_6 \delta \varepsilon_6 \} \, \mathrm{d}V \, \mathrm{d}t \\ & - \int_0^{T_0} \int_V \{ D_1 \delta E_1 + D_2 \delta E_2 + D_3 \delta E_3 \} \, \mathrm{d}V \, \mathrm{d}t \\ & + \int_0^{T_0} \int_S \{ t_1 \delta u_1 + t_2 \delta u_2 + t_3 \delta u_3 + q \delta \phi \} \, \mathrm{d}s \, \mathrm{d}t. \end{aligned} \quad (11)$$

Let eqn (11) be defined as the sum of four integrals:

$$0 = \delta K + \delta U + \delta E + \delta V. \tag{12}$$

The first integral denotes the virtual kinetic energy, the second denotes the virtual work done by internal forces, the third represents the contribution of the electric field, and the fourth denotes the virtual potential energy due to applied forces. In Hamilton's principle, it is assumed that the virtual displacements are zero at $t = 0, T_0 : \delta u_i|_0^{T_0} = 0$.

We begin with the first integral. Integrating the terms by parts to transfer all differentiations from the virtual displacements to their coefficients, we obtain

$$\begin{aligned}
\delta K = -\int_0^{T_0}\int_A \Bigg\{ & \left(I_1\ddot{u}_0 + I_2\ddot{\psi}_x - I_3\frac{\partial \ddot{w}_0}{\partial x}\right)\delta u_0 + \left(I_2\ddot{u}_0 + I_4\ddot{\psi}_x - I_5\frac{\partial \ddot{w}_0}{\partial x}\right)\delta\psi_x \\
& + \left[\frac{\partial}{\partial x}\left(I_3\ddot{u}_0 + I_5\ddot{\psi}_x - I_6\frac{\partial \ddot{w}_0}{\partial x}\right) + \frac{\partial}{\partial y}\left(I_3\ddot{v}_0 + I_5\ddot{\psi}_y - I_6\frac{\partial \ddot{w}_0}{\partial y}\right) + I_1\ddot{w}_0\right]\delta w_0 \\
& + \left(I_1\ddot{v}_0 + I_2\ddot{\psi}_y - I_3\frac{\partial \ddot{w}_0}{\partial y}\right)\delta v_0 + \left(I_2\ddot{v}_0 + I_4\ddot{\psi}_y - I_5\frac{\partial \ddot{w}_0}{\partial y}\right)\delta\psi_y \Bigg\}\,\mathrm{d}A\,\mathrm{d}t \\
& + \int_0^{T_0}\oint_S \left\{n_x\left(I_3\ddot{u}_0 + I_5\ddot{\psi}_x - I_6\frac{\partial \ddot{w}_0}{\partial x}\right) + n_y\left(I_3\ddot{v}_0 + I_5\ddot{\psi}_y - I_6\frac{\partial \ddot{w}_0}{\partial y}\right)\right\}\delta w_0\,\mathrm{d}s\,\mathrm{d}t,
\end{aligned} \tag{13}$$

where the mass inertia terms I_i are defined in the Appendix. Before proceeding with the second integral, we note that the transverse normal strain associated with the assumed displacement field (7) is zero. Hence, the admissible virtual strain is also zero, making the term $\delta\varepsilon_3\sigma_3 = 0$. On the other hand, σ_3 is assumed to be negligible by using the plane stress assumption. We have

$$\begin{aligned}
\delta U = -\int_0^{T_0}\int_A \Bigg\{ & \bar{N}_1\frac{\partial(\delta u_0)}{\partial x} + \bar{M}_1\frac{\partial(\delta\psi_x)}{\partial x} - \bar{P}_1\frac{\partial^2(\delta w_0)}{\partial x^2} \\
& + \bar{N}_2\frac{\partial(\delta v_0)}{\partial y} + \bar{M}_2\frac{\partial(\delta\psi_y)}{\partial x} - \bar{P}_2\frac{\partial^2(\delta w_0)}{\partial y^2} \\
& + \bar{N}_6\left(\frac{\partial(\delta u_0)}{\partial y} + \frac{\partial(\delta v_0)}{\partial x}\right) + \bar{M}_6\left(\frac{\partial(\delta\psi_x)}{\partial y} + \frac{\partial(\delta\psi_y)}{\partial x}\right) - 2\bar{P}_6\frac{\partial^2(\delta w_0)}{\partial x\,\partial y} \\
& + \bar{Q}_4\left(\delta\psi_y + \frac{\partial(\delta w_0)}{\partial y}\right) + \bar{Q}_5\left(\delta\psi_x + \frac{\partial(\delta w_0)}{\partial x}\right)\Bigg\}\,\mathrm{d}A\,\mathrm{d}t,
\end{aligned} \tag{14}$$

where $(\bar{N}_i, \bar{M}_i, \bar{P}_i)$ are the stress resultants

$$\bar{N}_i = \int_{-h/2}^{h/2}\sigma_i\,\mathrm{d}z \quad \bar{M}_i = \int_{-h/2}^{h/2}\sigma_i g_1(z)\,\mathrm{d}z \quad \bar{P}_i = \int_{-h/2}^{h/2}\sigma_i g_2(z)\,\mathrm{d}z, \quad i = 1,2,6, \tag{15a}$$

$$\bar{Q}_i = \int_{-h/2}^{h/2}\sigma_i\frac{\mathrm{d}g_1}{\mathrm{d}z}\,\mathrm{d}z, \quad i = 4,5. \tag{15b}$$

The overbars are used to indicate that resultants result from both the strain field and the electric field. Later, these effects will be separated out to indicate the nature of the coupling between the two. To obtain the Euler–Lagrange equations from (12), δU must be integrated by parts to transfer all differentiations from the virtual displacements to their coefficients. We obtain

$$\delta U = -\int_0^{T_0}\int_A \Bigg\{\Bigg[-\frac{\partial \bar{N}_1}{\partial x}\delta u_0 - \frac{\partial \bar{M}_1}{\partial x}\delta\psi_x - \frac{\partial^2 \bar{P}_1}{\partial x^2}\delta w_0\Bigg]$$
$$+\Bigg[-\frac{\partial \bar{N}_2}{\partial y}\delta v_0 - \frac{\partial \bar{M}_2}{\partial y}\delta\psi_y - \frac{\partial^2 \bar{P}_2}{\partial y^2}\delta w_0\Bigg]$$
$$+\Bigg[-\frac{\partial \bar{N}_6}{\partial y}\delta u_0 - \frac{\partial \bar{N}_6}{\partial x}\delta v_0 - \frac{\partial \bar{M}_6}{\partial y}\delta\psi_x - \frac{\partial \bar{M}_6}{\partial x}\delta\psi_y - 2\frac{\partial^2 \bar{P}_6}{\partial x\,\partial y}\delta w_0\Bigg]$$
$$+\Bigg[\bar{Q}_4\delta\psi_y - \frac{\partial \bar{Q}_4}{\partial y}\delta w_0\Bigg] + \Bigg[\bar{Q}_5\delta\psi_x - \frac{\partial \bar{Q}_5}{\partial x}\delta w_0\Bigg]\Bigg\}\,dA\,dt$$
$$-\oint_S \Bigg\{n_x\bar{N}_1\delta u_0 + n_x\bar{M}_1\delta\psi_x - \Bigg[\bar{P}_1\delta\left(\frac{\partial w_0}{\partial x}\right) - \frac{\partial \bar{P}_1}{\partial x}\delta w_0\Bigg]n_x$$
$$+n_y\bar{N}_2\delta v_0 + n_y\bar{M}_2\delta\psi_y - \Bigg[\bar{P}_2\delta\left(\frac{\partial w_0}{\partial y}\right) - \frac{\partial \bar{P}_2}{\partial y}\delta w_0\Bigg]n_y$$
$$+n_x\bar{N}_6\delta v_0 + n_y\bar{N}_6\delta u_0 + n_y\bar{M}_6\delta\psi_x + n_x\bar{M}_6\delta\psi_y$$
$$-\Bigg[\bar{P}_6\delta\left(\frac{\partial w_0}{\partial y}\right)n_x + \bar{P}_6\delta\left(\frac{\partial w_0}{\partial x}\right)n_y - \left(\frac{\partial \bar{P}_6}{\partial x}n_y + \frac{\partial \bar{P}_6}{\partial y}n_x\right)\delta w_0\Bigg]$$
$$+n_y\bar{Q}_4\delta w_0 + n_x\bar{Q}_5\delta w_0\Bigg\}\,ds. \tag{16}$$

Similarly, the third integral can be written, in view of eqns (3) and (9), as

$$\delta E = -\int_0^{T_0}\int_V \left(D_1\frac{\partial\delta\phi}{\partial x} + D_2\frac{\partial\delta\phi}{\partial y} + D_3\frac{\partial\delta\phi}{\partial z}\right)dV\,dt$$
$$= -\int_0^{T_0}\sum_{k=1}^{m}\Bigg[\int_A\Bigg\{\sum_{j=1}^{n}P_\alpha^{jk}\frac{\partial(\delta\varphi_j^k)}{\partial x_\alpha} + \sum_{j=1}^{n}G_3^{jk}\delta\varphi_j^k\Bigg\}dA\Bigg]dt$$
$$= -\int_0^{T_0}\Bigg\{\sum_{k=1}^{m}\Bigg[\oint_S\sum_{j=1}^{n}P_\alpha^{jk}n_\alpha\delta\varphi_j^k\,ds - \int_A\sum_{j=1}^{n}\left(\frac{\partial P_\alpha^{jk}}{\partial x_\alpha} - G_3^{jk}\right)\delta\varphi_j^k\,dA\Bigg]\Bigg\}dt, \tag{17a}$$

where ($\alpha = 1, 2$) and

$$P_\alpha^{jk} = \int_{z_{k-1}}^{z_k} D_\alpha f_j(z)\,dz, \quad G_3^{jk} = \int_{z_{k-1}}^{z_k} D_3\frac{df_j}{dz}dz. \tag{17b}$$

Substituting expressions from eqns (13), (16), and (17) into (12), and collecting the coefficients of $(\delta u_0, \delta v_0, \delta w_0, \delta\psi_x, \delta\psi_y, \delta\varphi_j^k)$ and setting them to zero, we obtain the Euler–Lagrange equations:

$$\delta u_0: \quad -\left(I_1\ddot{u}_0 + I_2\ddot{\psi}_x - I_3\frac{\partial\ddot{w}_0}{\partial x}\right) + \frac{\partial \bar{N}_1}{\partial x} + \frac{\partial \bar{N}_6}{\partial y} = 0, \tag{18a}$$

$$\delta v_0: \quad -\left(I_1\ddot{v}_0 + I_2\ddot{\psi}_y - I_3\frac{\partial\ddot{w}_0}{\partial y}\right) + \frac{\partial \bar{N}_2}{\partial y} + \frac{\partial \bar{N}_6}{\partial x} = 0, \tag{18b}$$

$$\delta w_0: \quad -\Bigg[I_1\ddot{w}_0 + \frac{\partial}{\partial x}\left(I_3\ddot{u}_0 + I_5\ddot{\psi}_x - I_6\frac{\partial\ddot{w}_0}{\partial x}\right) + \frac{\partial}{\partial y}\left(I_3\ddot{v}_0 + I_5\ddot{\psi}_y - I_6\frac{\partial\ddot{w}_0}{\partial y}\right)\Bigg]$$

$$+\frac{\partial^2 \bar{P}_1}{\partial x^2}+\frac{\partial^2 \bar{P}_2}{\partial y^2}+2\frac{\partial^2 \bar{P}_6}{\partial x\,\partial y}+\frac{\partial \bar{Q}_4}{\partial y}+\frac{\partial \bar{Q}_5}{\partial x}=0, \tag{18c}$$

$$\delta\psi_x: \quad -\left[\left(I_2\ddot{u}_0+I_4\ddot{\psi}_x-I_5\frac{\partial \ddot{w}_0}{\partial x}\right)\right]+\frac{\partial \bar{M}_1}{\partial x}+\frac{\partial \bar{M}_6}{\partial y}-\bar{Q}_5=0, \tag{18d}$$

$$\delta\psi_y: \quad -\left[\left(I_2\ddot{v}_0+I_4\ddot{\psi}_y-I_5\frac{\partial \ddot{w}_0}{\partial y}\right)\right]+\frac{\partial \bar{M}_2}{\partial y}+\frac{\partial \bar{M}_6}{\partial x}-\bar{Q}_4=0, \tag{18e}$$

$$\delta\varphi_j^k: \quad \frac{\partial P_\alpha^{jk}}{\partial x_\alpha}-G_3^{jk}=0 \quad (\alpha=1,2). \tag{18f}$$

Now it is useful to decompose the stress resultants $\bar{N}_i$, $\bar{M}_i$, $\bar{P}_i$, $\bar{Q}_i$ into two parts. The first part is that which would be given if the piezoelectric effect was not present. The second part results due to the presence of the piezoelectric lamina. Recall the constitutive relationships and strain relationships (excluding piezoelectric terms):

$$\begin{Bmatrix}\sigma_1\\ \sigma_2\\ \sigma_6\end{Bmatrix}=\begin{bmatrix}c_{11} & c_{12} & 0\\ c_{12} & c_{22} & 0\\ 0 & 0 & c_{66}\end{bmatrix}\begin{Bmatrix}\dfrac{\partial u_0}{\partial x}\\ \dfrac{\partial v_0}{\partial y}\\ \dfrac{\partial u_0}{\partial y}+\dfrac{\partial v_0}{\partial x}\end{Bmatrix}+g_1\begin{bmatrix}c_{11} & c_{12} & 0\\ c_{12} & c_{22} & 0\\ 0 & 0 & c_{66}\end{bmatrix}\begin{Bmatrix}\dfrac{\partial \psi_x}{\partial x}\\ \dfrac{\partial \psi_y}{\partial y}\\ \dfrac{\partial \psi_x}{\partial y}+\dfrac{\partial \psi_y}{\partial x}\end{Bmatrix}$$

$$-g_2\begin{bmatrix}c_{11} & c_{12} & 0\\ c_{12} & c_{22} & 0\\ 0 & 0 & c_{66}\end{bmatrix}\begin{Bmatrix}\dfrac{\partial^2 w_0}{\partial x^2}\\ \dfrac{\partial^2 w_0}{\partial y^2}\\ 2\dfrac{\partial^2 w_0}{\partial x\,\partial y}\end{Bmatrix}, \tag{19a}$$

$$\begin{Bmatrix}\sigma_4\\ \sigma_5\end{Bmatrix}=\frac{dg_1}{dz}\begin{bmatrix}c_{44} & 0\\ 0 & c_{55}\end{bmatrix}\begin{Bmatrix}\psi_y+\dfrac{\partial w_0}{\partial y}\\ \psi_x+\dfrac{\partial w_0}{\partial x}\end{Bmatrix}. \tag{19b}$$

As described above, the stress resultants are decomposed as:

$$\bar{N}_i=N_i+N_i^{\mathrm{P}}, \tag{20a}$$

$$\bar{M}_i=M_i+M_i^{\mathrm{P}}, \tag{20b}$$

$$\bar{P}_i=P_i+P_i^{\mathrm{P}}, \tag{20c}$$

$$\bar{Q}_i=Q_i+Q_i^{\mathrm{P}}, \tag{20d}$$

where superscripts P denote resultants due to piezoelectric effects, and N_i, M_i, P_i, and Q_i are the usual stress resultants, which are related to the strains through the following laminate constitutive relationships:

$$\begin{Bmatrix} N_1 \\ N_2 \\ N_3 \\ M_1 \\ M_2 \\ M_3 \\ P_1 \\ P_2 \\ P_6 \end{Bmatrix} = \begin{bmatrix} A_{11} & A_{12} & 0 & \bar{A}_{11} & \bar{A}_{12} & 0 & \bar{\bar{A}}_{11} & \bar{\bar{A}}_{12} & 0 \\ & A_{22} & 0 & \bar{A}_{12} & \bar{A}_{22} & 0 & \bar{\bar{A}}_{12} & \bar{\bar{A}}_{22} & 0 \\ & & A_{66} & 0 & 0 & \bar{A}_{66} & 0 & 0 & \bar{\bar{A}}_{66} \\ & & & B_{11} & B_{12} & 0 & \bar{B}_{11} & \bar{B}_{12} & 0 \\ & & & & B_{22} & 0 & \bar{B}_{12} & \bar{B}_{22} & 0 \\ & & & & & B_{66} & 0 & 0 & \bar{B}_{66} \\ & \text{symmetric} & & & & & D_{11} & D_{12} & 0 \\ & & & & & & & D_{22} & 0 \\ & & & & & & & & D_{66} \end{bmatrix} \times \begin{Bmatrix} \dfrac{\partial u_0}{\partial x} \\ \dfrac{\partial v_0}{\partial y} \\ \dfrac{\partial u_0}{\partial y} + \dfrac{\partial v_0}{\partial x} \\ \dfrac{\partial \psi_x}{\partial x} \\ \dfrac{\partial \psi_y}{\partial y} \\ \dfrac{\partial \psi_x}{\partial y} + \dfrac{\partial \psi_y}{\partial x} \\ -\dfrac{\partial^2 w_0}{\partial x^2} \\ -\dfrac{\partial^2 w_0}{\partial y^2} \\ -2\dfrac{\partial^2 w_0}{\partial x \partial y} \end{Bmatrix}, \tag{21a}$$

$$\begin{Bmatrix} Q_4 \\ Q_5 \end{Bmatrix} = \begin{bmatrix} F_{44} & 0 \\ 0 & F_{55} \end{bmatrix} \begin{Bmatrix} \psi_y + \dfrac{\partial w_0}{\partial y} \\ \psi_x + \dfrac{\partial w_0}{\partial x} \end{Bmatrix}, \tag{21b}$$

where the laminate stiffnesses A_{ij}, B_{ij} and so on are defined in the Appendix. To evaluate the piezoelectric stress resultants recall the approximation for the potential function and the terms contributing to the stress components due to the piezoelectric effect. These stresses are given as

$$\sigma_1^{\mathrm{P}} = e_{31} \sum_{j=1}^{n} \frac{\mathrm{d}f_j}{\mathrm{d}z} \varphi_j, \quad \sigma_4^{\mathrm{P}} = e_{24} \sum_{j=1}^{n} f_j \frac{\partial \varphi_j}{\partial y},$$

$$\sigma_2^{\mathrm{P}} = e_{32} \sum_{j=1}^{n} \frac{\mathrm{d}f_j}{\mathrm{d}z} \varphi_j, \quad \sigma_5^{\mathrm{P}} = e_{15} \sum_{j=1}^{n} f_j \frac{\partial \varphi_j}{\partial x}, \quad \sigma_6^{\mathrm{P}} = 0. \tag{22}$$

Note that these are stresses defined at the layerwise element level. Also it is clear that the piezoelectric contribution to the inplane shear stress σ_6 is zero when the piezoelectric material axes are coincident with the laminate axes as considered here. Now the stress resultants due to the piezoelectric lamina can be defined as

$$N_1^{\mathrm{P}} = \sum_{k=1}^{m} e_{31}^k \left(\sum_{j=1}^{n} \beta_1^{jk} \varphi_j^k \right), \quad N_2^{\mathrm{P}} = \sum_{k=1}^{m} e_{32}^k \left(\sum_{j=1}^{n} \beta_1^{jk} \varphi_j^k \right), \quad N_6^{\mathrm{P}} = 0, \tag{23a}$$

$$M_1^{\mathrm{P}} = \sum_{k=1}^{m} e_{31}^k \left(\sum_{j=1}^{n} \beta_2^{jk} \varphi_j^k \right), \quad M_2^{\mathrm{P}} = \sum_{k=1}^{m} e_{32}^k \left(\sum_{j=1}^{n} \beta_2^{jk} \varphi_j^k \right), \quad M_6^{\mathrm{P}} = 0, \tag{23b}$$

$$P_1^{\mathrm{P}} = \sum_{k=1}^{m} e_{31}^k \left(\sum_{j=1}^{n} \beta_3^{jk} \varphi_j^k \right), \quad P_2^{\mathrm{P}} = \sum_{k=1}^{m} e_{32}^k \left(\sum_{j=1}^{n} \beta_3^{jk} \varphi_j^k \right), \quad P_6^{\mathrm{P}} = 0, \tag{23c}$$

$$Q_4^{\mathrm{P}} = \sum_{k=1}^{m} e_{24}^k \left(\sum_{j=1}^{n} \alpha_4^{jk} \frac{\partial \varphi_j^k}{\partial y} \right), \quad Q_5^{\mathrm{P}} = \sum_{k=1}^{m} e_{15}^k \left(\sum_{j=1}^{n} \alpha_4^{jk} \frac{\partial \varphi_j^k}{\partial x} \right). \tag{23d}$$

Note that m corresponds to the number of laminae in the laminate and n corresponds to the number of nodes used to model a particular lamina. The appendix contains the definitions for β_1^{jk}, β_2^{jk}, β_3^{jk}, and α_4^{jk} which simply result from integrating through the thickness direction. With these definitions for stress resultants, the Euler–Lagrange equations are now written in terms of the mechanical and piezoelectric resultants:

$$\delta u_0 : \frac{\partial N_1}{\partial x} + \frac{\partial N_6}{\partial y} + \sum_{k=1}^{m} e_{31}^k \left(\sum_{j=1}^{n} \beta_1^{jk} \frac{\partial \varphi_j^k}{\partial x} \right) = I_1 \ddot{u}_0 + I_2 \ddot{\psi}_x - I_3 \frac{\partial \ddot{w}_0}{\partial x}, \tag{24a}$$

$$\delta v_0 : \frac{\partial N_2}{\partial y} + \frac{\partial N_6}{\partial x} + \sum_{k=1}^{m} e_{32}^k \left(\sum_{j=1}^{n} \beta_1^{jk} \frac{\partial \varphi_j^k}{\partial y} \right) = I_1 \ddot{v}_0 + I_2 \ddot{\psi}_y - I_3 \frac{\partial \ddot{w}_0}{\partial y}, \tag{24b}$$

$$\begin{aligned} \delta w_0 : \frac{\partial^2 P_1}{\partial x^2} + \frac{\partial^2 P_2}{\partial y^2} + 2\frac{\partial^2 P_6}{\partial x \partial y} + \frac{\partial Q_4}{\partial y} + \frac{\partial Q_5}{\partial x} + \sum_{k=1}^{m} \left[e_{31}^k \sum_{j=1}^{n} \beta_3^{jk} \frac{\partial^2 \varphi_j^k}{\partial x^2} + e_{32}^k \sum_{j=1}^{n} \beta_3^{jk} \frac{\partial^2 \varphi_j^k}{\partial y^2} \right] \\ + \sum_{k=1}^{m} \left[e_{24}^k \sum_{j=1}^{n} \alpha_4^{jk} \frac{\partial^2 \varphi_j^k}{\partial y^2} + e_{15}^k \sum_{j=1}^{n} \alpha_4^{jk} \frac{\partial^2 \phi_j^k}{\partial x^2} \right] \\ = I_1 \ddot{w}_0 + \frac{\partial}{\partial x} \left[I_3 \ddot{u}_0 + I_5 \ddot{\psi}_x - I_6 \frac{\partial \ddot{w}_0}{\partial x} \right] + \frac{\partial}{\partial y} \left[I_3 \ddot{v}_0 + I_5 \ddot{\psi}_y - I_6 \frac{\partial \ddot{w}_0}{\partial y} \right], \end{aligned} \tag{24c}$$

$$\begin{aligned} \delta \psi_x : \frac{\partial M_1}{\partial x} + \frac{\partial M_6}{\partial y} - Q_5 + \sum_{k=1}^{m} \left[e_{31}^k \left(\sum_{j=1}^{n} \beta_2^{jk} \frac{\partial \varphi_j^k}{\partial x} \right) - e_{15}^k \left(\sum_{j=1}^{n} \alpha_4^{jk} \frac{\partial \varphi_j^k}{\partial x} \right) \right] \\ = I_2 \ddot{u}_0 + I_4 \ddot{\psi}_x - I_5 \frac{\partial \ddot{w}_0}{\partial x}, \end{aligned} \tag{24d}$$

$$\begin{aligned} \delta \psi_y : \frac{\partial M_2}{\partial y} + \frac{\partial M_6}{\partial x} - Q_4 + \sum_{k=1}^{m} \left[e_{32}^k \left(\sum_{j=1}^{n} \beta_2^{jk} \frac{\partial \varphi_j^k}{\partial y} \right) - e_{15}^k \left(\sum_{j=1}^{n} \alpha_4^{jk} \frac{\partial \varphi_j^k}{\partial x} \right) \right] \\ = I_2 \ddot{v}_0 + I_4 \ddot{\psi}_y - I_5 \frac{\partial \ddot{w}_0}{\partial y}. \end{aligned} \tag{24e}$$

Equations (24) are subject to the following essential boundary conditions (EBC) and the natural boundary conditions (NBC):

EBC NBC

$$u_0 \quad \text{or} \quad n_x\left[N_1+\sum_{k=1}^{m} e_{31}^k\left(\sum_{j=1}^{n}\beta_1^{jk}\varphi_j^k\right)\right]+N_6 n_y \tag{25a}$$

$$v_0 \quad \text{or} \quad n_y\left[N_2+\sum_{k=1}^{m} e_{32}^k\left(\sum_{j=1}^{n}\beta_1^{jk}\varphi_j^k\right)\right]+N_6 n_x \tag{25b}$$

$$w_0 \quad \text{or} \quad n_x\left(I_3\ddot{u}_0+I_5\ddot{\psi}_x-I_6\frac{\partial\ddot{w}_0}{\partial x}\right)+n_y\left(I_3\ddot{v}_0+I_5\ddot{\psi}_y-I_6\frac{\partial\ddot{w}_0}{\partial y}\right)+Q_n \tag{25c}$$

$$\delta\left(\frac{\partial w_0}{\partial x}\right) \quad \text{or} \quad n_x\left[P_1+\sum_{k=1}^{m} e_{31}^k\left(\sum_{j=1}^{n}\beta_3^{jk}\varphi_j^k\right)\right]+n_y P_6 \tag{25d}$$

$$\delta\left(\frac{\partial w_0}{\partial y}\right) \quad \text{or} \quad n_y\left[P_2+\sum_{k=1}^{m} e_{32}^k\left(\sum_{j=1}^{n}\beta_3^{jk}\varphi_j^k\right)\right]+n_x P_6 \tag{25e}$$

$$\delta\psi_x \quad \text{or} \quad -n_x\left[M_1+\sum_{k=1}^{m} e_{31}^k\left(\sum_{j=1}^{n}\beta_2^{jk}\varphi_j^k\right)\right]-n_y M_6 \tag{25f}$$

$$\delta\psi_y \quad \text{or} \quad -n_y\left[M_2+\sum_{k=1}^{m} e_{32}^k\left(\sum_{j=1}^{n}\beta_2^{jk}\varphi_j^k\right)\right]-n_x M_6 \tag{25g}$$

where

$$Q_n=-n_x\left[\frac{\partial P_1}{\partial x}+\sum_{k=1}^{m} e_{31}^k\left(\sum_{j=1}^{n}\beta_3^{jk}\frac{\partial\varphi_j^k}{\partial x}\right)\right]-n_y\left[\frac{\partial P_2}{\partial y}+\sum_{k=1}^{m} e_{32}^k\left(\sum_{j=1}^{n}\beta_3^{jk}\frac{\partial\varphi_j^k}{\partial y}\right)\right]$$
$$-n_x\frac{\partial P_6}{\partial y}-n_y\frac{\partial P_6}{\partial x}-n_y\left[Q_4+\sum_{k=1}^{m} e_{24}^k\left(\sum_{j=1}^{n}\alpha_4^{jk}\frac{\partial\varphi_j^k}{\partial y}\right)\right]-n_x\left[Q_5+\sum_{k=1}^{m} e_{15}^k\left(\sum_{j=1}^{n}\alpha_4^{jk}\frac{\partial\varphi_j^k}{\partial x}\right)\right]. \tag{26}$$

Next we discuss the charge boundary condition from the third and fourth integrals. In most circumstances, the potential on the surfaces of the piezoelectric is specified and the charge density q per unit area is found in a postcalculation. This is described here in detail not only because it is a necessary step for the theory presented here, but also because laminae may be used for sensors as well as actuators. In the case of sensors, strains and or strain rate measurements may be made by measuring charge, currents, or voltages on the major surfaces of the piezoelectric lamina [see, e.g. Lee (1990), Lee and Moon (1990), and Tzou *et al.* (1993)]. These measurements are based on the fact that at a dielectric–conductor interface, $\mathbf{D}\cdot\hat{\mathbf{n}}=q$, where $\hat{\mathbf{n}}$ is the outward unit normal to the conductor surface. This necessary condition arises naturally in the formulation here and gives physical insight into the assembly process.

To begin, the charge term in δV and all of δE for the kth lamina is rewritten here as

$$\int_0^{T_0}\int_{S^k} q\delta\phi\,\mathrm{d}s\,\mathrm{d}t-\int_0^{T_0}\int_{V^k} D_i(\delta\phi)_{,i}\,\mathrm{d}V\,\mathrm{d}t=0, \tag{27}$$

where S^k and V^k correspond to the surface and volume of the kth lamina. The surface integral is composed of three parts: the major surfaces S_1^k (bottom), S_2^k (top), and edges of the plate S_3^k. On the major surfaces S_1^k and S_2^k at $z=z_k$ and $z=z_{k+1}$ respectively, the potential ϕ is given as

$$\phi(z_k) = f^k_{j=1}(z_k)\phi^k_{j=1} = \phi^k_{j=1},$$
$$\phi(z_{k+1}) = f^k_{j=n}(z_{k+1})\phi^k_{j=n} = \phi^k_{j=n}. \tag{28}$$

Each mathematical layer or lamina has n nodes and assembly is accomplished by setting

$$\phi^k_n = \phi^{k+1}_1. \tag{29}$$

This is the normal process of assembly described in books on the finite element method [see Reddy (1993)] where φ^k_j is called a primary variable. A secondary variable or flux-type term is also defined, and in this case it corresponds to the normal component of the electric displacement. If the interface between mathematical layers is a conductor–dielectric interface, then a charge q can exist there due to a combination of applied mechanical as well as electrical loadings.

Returning to the charge equations (27), substituting the approximation for the potential function, and summing over all laminae, the following equation is given:

$$0 = \int_0^{T_0}\left[\sum_{k=1}^{m}\left\{\int_{S^k}\left(q\sum_{j=1}^{n} f_j\delta\varphi^k_j\right)\mathrm{d}s - \int_{V^k}\left[\sum_{j=1}^{n}\left(D_1 f_j\frac{\partial\delta\varphi^k_j}{\partial x} + D_2 f_j\frac{\partial\delta\varphi^k_j}{\partial y} + D_3\frac{\mathrm{d}f_j}{\mathrm{d}z}\delta\varphi^k_j\right)\right]\mathrm{d}V\right\}\right]\mathrm{d}t. \tag{30}$$

The volume integral in the above equation is selectively integrated by parts so that the appropriate boundary conditions are obtained. The surface integral is now taken in three parts over surfaces S^k_1, S^k_2, and S^k_3:

$$0 = \int_0^{T_0}\left\{\sum_{k=1}^{m}\left[\int_{S^k_1} q^k_1\delta\phi^k_1\,\mathrm{d}S^k_1 + \int_{S^k_2} q^k_2\delta\phi^k_n\,\mathrm{d}S^k_2 + \oint_C\sum_{j=1}^{n} q_{jk}\delta\varphi^k_j\,\mathrm{d}c - \int_A\sum_{j=1}^{n} P^{jk}_a\frac{\partial}{\partial x_a}(\delta\varphi^k_j)\,\mathrm{d}A - \int_S n_3 D_3\sum_{j=1}^{n} f_j\delta\varphi^k_j\big|^{z_{k+1}}_{z_k}\mathrm{d}S + \int_V\frac{\partial D_3}{\partial z}\sum_{j=1}^{n} f_j\delta\varphi^k_j\,\mathrm{d}V\right]\right\}\mathrm{d}t. \tag{31}$$

Using the same definitions as given previously in this paper for the charge resultants, and defining a new lamina charge as

$$q_{jk} = \int_{z_k}^{z_{k+1}} q f_j(z)\,\mathrm{d}z, \tag{32}$$

a slightly different form for the governing charge equations is obtained:

$$0 = \int_0^{T_0}\sum_{k=1}^{m}\left\{\int_{S^k_1}(q^k_1 + n_3 D_3)\delta\phi^k_1\,\mathrm{d}S^k_1 + \int_{S^k_2}(q^k_2 - n_3 D_3)\delta\phi^k_n\,\mathrm{d}S^k_2 + \oint_{C^k}\sum_{j=1}^{n}(q_{jk} - P^{jk}_\alpha n_\alpha)\delta\varphi^k_j\,\mathrm{d}c + \int_A\sum_{j=1}^{n}\left(\frac{\partial P^{jk}_\alpha}{\partial x_\alpha} + \bar{G}^{jk}_3\right)\delta\varphi^k_j\,\mathrm{d}A\right\}, \tag{33}$$

where $\alpha = 1, 2$

$$\bar{G}^{jk}_3 = \int_{z_k}^{z_{k+1}}\frac{\partial D_3}{\partial z} f_j\,\mathrm{d}z. \tag{34}$$

Notice the difference in the definitions for G^{jk}_3 and $\bar{G}^{jk}_3$. While the resulting equations look

different because of the different definitions for G_3^{jk} and $\bar{G}_3^{jk}$, they are equivalent since differences arise due to integration by parts only. However, from this modified form, it is possible to identify boundary conditions that should be satisfied. Although this is an approximate formulation, the boundary conditions are essentially identical to those obtained using a linear theory with no approximations. It is also noted that G_3^{jk} is obtained from the weak form and combined with $\partial P_\alpha^{jk}/\partial x_\alpha$ which is a term representing an approximation to the strong form of the governing equation. Because of this fact, G_3^{jk} is easier to work with in terms of actual implementation because it requires less differentiability of the interpolation functions $f_j(z)$. In example problems studied here, the equations with G_3^{jk} are used. This latter description was derived here to indicate that all the essential physics concerning the charge equations of electrostatics are embedded in this approximate theory and also to discuss briefly how the charge boundary conditions given here relate to previously published work concerning piezoelectric laminae as sensors.

3. DISCUSSION OF LAMINA SENSORS

Next we make the connection between the present theory and two previously published theories (Lee, 1990 and Tzou *et al.*, 1993), concerning piezoelectric laminae as sensors. For sensor purposes, Tzou *et al.* (1993) take the lamina to be in an open-circuit condition and assume that the charge equations, which correspond to the divergence of the electric displacements, reduce to the divergence of D_3 with respect to x_3 (the thickness coordinate) for thin laminates. In the present theory, this corresponds to assuming that for the kth lamina, the following equation is automatically satisfied:

$$\frac{\partial P_1^{jk}}{\partial x_1} + \frac{\partial P_2^{jk}}{\partial x_2} = 0. \tag{35}$$

The extent to which this equation is not satisfied depends upon the thickness of the lamina and on how much shear stress the lamina is subjected to. Based on this assumption, the remaining portion of the charge equation is

$$G_3^{jk} = \int_{z_{k-1}}^{z_k} D_3 \frac{\mathrm{d}f_j}{\mathrm{d}z}\,\mathrm{d}z = 0. \tag{36}$$

Using the constitutive relationship for D_3, we obtain

$$G_3^{jk} = \int_{z_{k-1}}^{z_k} \left\{ e_{31}\varepsilon_1 + e_{32}\varepsilon_2 - k_{33}\left(\sum_{l=1}^{n} \frac{\mathrm{d}f_l}{\mathrm{d}z}\phi_l\right)\right\}\frac{\mathrm{d}f_j}{\mathrm{d}z}\,\mathrm{d}z = 0. \tag{37}$$

The connection of this assumption to modeling is through the selection of interpolation functions $f_j(z)$. Based on the thin lamina assumption, one linear interpolation function is used for the piezoelectric lamina. In the variational formulation, the potential at the top and bottom of the laminae is not specified because of the open circuit sensor condition and therefore we conclude that two charge equations corresponding to two primary nodal variables must be satisfied. This corresponds to letting $j = 1$ and 2 in eqn (37). Substituting the linear interpolation functions into eqn (37), and integrating through the thickness of the kth lamina gives

$$V_3^k = \frac{1}{k_{33}} \int_{z_{k-1}}^{z_k} (e_{31}\varepsilon_1 + e_{32}\varepsilon_2)\,\mathrm{d}z, \tag{38}$$

where $V_3^k = (\phi_1^k - \phi_2^k)$. The same equation is given for both $j = 1$ and 2. Here, we interpret the left-hand side as the local voltage induced by the strain field on the right-hand side.

Equation (38) corresponds to eqn (6) in the paper by Tzou *et al.* (1993). An alternative approach is to close the circuit so that the charge flow can be measured. The total charge Q^k is that given by

$$Q^k(t) = \int_{S_{12}^k} D_3|_{z=z_k}\,\mathrm{d}S_{12}^k + \int_{S_{12}^k} D_3|_{z=z_{k+1}}\,\mathrm{d}S_{12}^k = \int (q_1^k + q_2^k)\,\mathrm{d}S_{12}^k, \tag{39}$$

where $S_{12}^k = S_1^k \cap S_2^k$ and is called the effective surface electrode [see Lee (1990)]. So that the charge signal can be directly related to mechanical deformation, the major surfaces of the lamina are short-circuited, and piezoelectric laminae are modeled with one linear element. As in the previous sensor discussion above, the charge signal may still contain effects due to non-linear variations (with respect to z) of the potential interior to the lamina major surfaces. While this is probably more correct, this effect is likely to be insignificant if the piezoelectric lamina is thin, as was considered by Lee (1990). However, it should be noted that it is not possible, from the work of Lee (1990), to model effects which arise due to some piezoelectric lamina surfaces not being covered with electrodes. In this case, both continuity of potential and the normal component of electric displacement must be enforced between the lamina and whatever it is adjacent to. If for instance the lamina is exposed to free space, then a differential equation on the electric potential ϕ^f for free space should be solved [see Tiersten (1981)]. Then the potential corresponding to material points on the surface should match the potential for free space. In the case of the present theory, the deformations are assumed to be small and therefore the present coordinates of the laminate can be taken as the undeformed coordinates. It is possible to incorporate this into the current model in addition to other types of loading conditions such as interdigitated electrodes [see Hagood *et al.* (1993)]. Traditionally, most piezoelectric applications in smart structures have fields applied through the thickness direction of the lamina. In these cases, assuming that the electric field is constant through the thickness is a good approximation. However, it is impossible to use these types of models to analyse conditions such as those present due to interdigitated surface electrodes.

4. RESULTS

4.1. *Analytical solution*

In this section, the equations derived in Section 2 are used to study static deflections and natural frequencies of symmetric, simply supported, laminated plates with piezoelectric laminae. Various plate span ratios and plate thickness studies are given here. To investigate the effects of modeling the potential function, results are also presented for classical plate theory (CPT) and for the third-order shear deformation theory using the induced strains method. Although the charge equations of electrostatics have been added to the system of governing equations for this hybrid theory, it is still possible to find the Navier solution for simply supported, symmetric cross-ply plates. The solution for simply supported cross-ply laminates has the following form:

$$\begin{aligned} w &= \sum_m \sum_n W_{mn} \sin mx \sin ny, \\ \psi_x &= \sum_m \sum_n \psi_{mn}^x \cos mx \sin ny, \\ \psi_y &= \sum_m \sum_n \psi_{mn}^y \sin mx \cos ny, \\ \phi &= \sum_m \sum_n \phi_{mn} \sin mx \sin ny. \end{aligned} \tag{40}$$

For the particular examples considered here, the inplane displacement field (u_0, v_0) is uncoupled from the out-of-plane displacement field (w_0, ψ_x, ψ_y). This is briefly discussed

here. Recall that for symmetric laminates, the constitutive elements $\bar{A}$, $\bar{\bar{A}}$ are zero and therefore coupling cannot occur mechanically. Therefore the only remaining source of coupling is through the potential function. The particular source of coupling [see eqns (24a) and (24b)] is only possible through the terms

$$\sum_{k=1}^{m} e_{31}^{k}\left(\sum_{j=1}^{n}\beta_1^{jk}\frac{\partial\varphi_j^k}{\partial x}\right),\quad \sum_{k=1}^{m} e_{32}^{k}\left(\sum_{j=1}^{n}\beta_1^{jk}\frac{\partial\varphi_j^k}{\partial y}\right). \tag{41}$$

To investigate further, consider two adjacent mathematical layers below the $z = 0$ plane and its symmetric counterparts above the $z = 0$ plane. Let each mathematical layer be modeled using linear Lagrange elements. During the assembly process, the common node between adjacent elements will have, say ϕ^l as a global variable name and assembly will give a term corresponding to this common node as

$$(e_{31}^{k}\beta_1^{2k}+e_{31}^{k+1}\beta_1^{1(k+1)})\frac{\partial\phi^l}{\partial x}. \tag{42}$$

In the case of linear elements we have

$$\beta_1^{2k} = -\beta_1^{1(k+1)} = 1. \tag{43}$$

Therefore the assembly process gives

$$(e_{31}^{k}-e_{31}^{k+1})\frac{\partial\phi^l}{\partial x}. \tag{44}$$

This illustrates the possibility for coupling. If two adjacent mathematical layers are composed of different piezoelectric materials, say e_{31}^{k} and e_{31}^{k+1}, and the potential is not specified at this interface, then $e_{31}^{k}-e_{31}^{k+1}\neq 0$ and the inplane displacement field is coupled with the out-of-plane displacement field through the potential function. However, if the two layers are composed of the same piezoelectric material, then coupling will not occur. To summarize, assembly is concerned with adding the effects of adjacent elements at a node. When one piezoelectric element or lamina is not adjacent to another, then the potential is typically applied there. This corresponds to the forcing term that goes to the right-hand side of the governing equations.

Now consider the symmetry of the laminate and applied voltages. For plates, piezoelectric laminae can be utilized as benders or pushers. Benders utilize symmetry of both the laminate and the applied voltages. This naturally falls out of the present theory during assembly. Benders induce an antisymmetric axial stress field in the laminate, thus giving a zero net inplane force resultant but a non-zero moment. In this case, the inplane displacement field is zero because the forcing terms that go to the right-hand side of eqns (24a) and (24b) add to zero for similar reasons to those described for adjacent elements during assembly.

4.2. *Discussion of the results*

The phrase 'strain induced method' refers to a method in which the piezoelectric effect is included in the mechanical constitutive relationships only, and the charge equations of electrostatics are ignored. Results from the present study indicate that for PVDF and PZT, the above assumption is valid for a large range of plate span ratios and piezoelectric thickness ratios. However, as the plate becomes thicker (within the range of validity of shear deformation theories), modeling of the electric potential becomes more important,

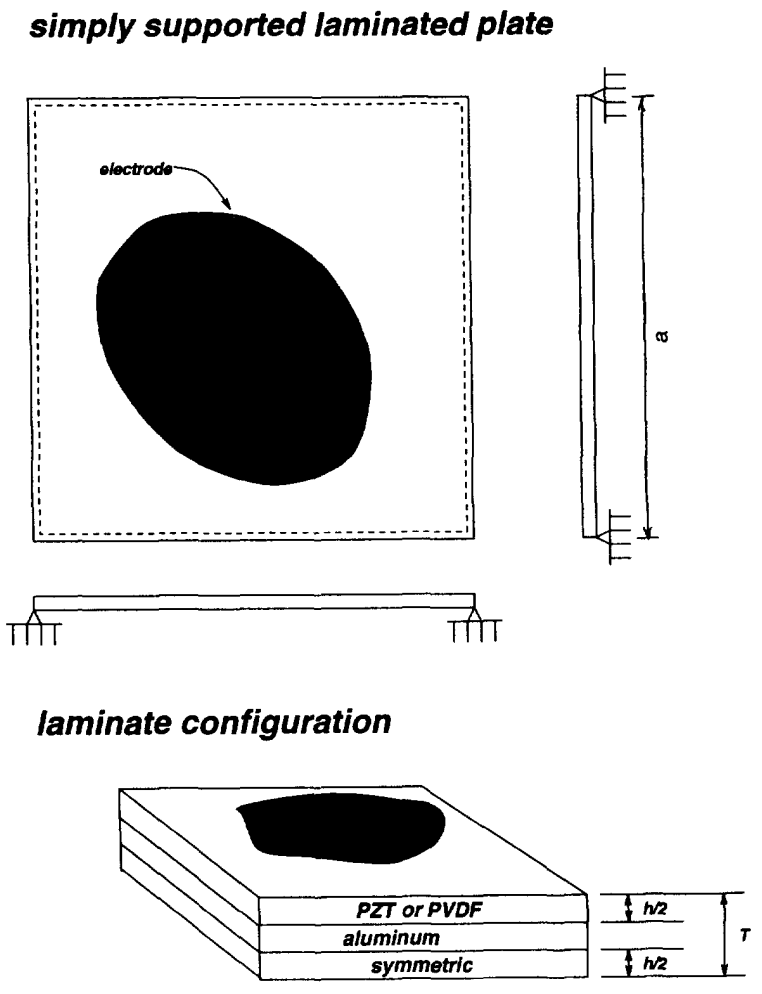

Fig. 1. Geometry and laminate configurations.

especially for plates with a high piezoelectric thickness ratio h/T (see Fig. 1). The material properties used in the examples are given in the Appendix. Also, it should be noted that results correspond to the layerwise discretization of one quadratic element per piezoelectric layer.

In general, PVDF laminates show a high degree of insensitivity to the modeling of the electric potential, as indicated in Fig. 2. The transverse deflection at the center of the plate is identical for all three theories considered here: CPT, strain induced third-order plate theory, and third-order theory including electric potential. These deflections are due to a uniform unit potential applied across each PVDF layer in order to induce bending. In this case there are two factors that affect the trends. As the PVDF lamina becomes thicker the effective electric field is reduced, thereby inducing less strains and ultimately reduced deflections. However, due to the fact that PVDF is mechanically weaker than the aluminium that it replaces, as the piezoelectric thickness ratio increases, the magnitude of the resulting deflections increases. The relative importance of these two effects is reversed in laminates containing PZT; PZT is mechanically as strong as aluminum and therefore as the PZT layers become thicker the effective E fields are reduced, thereby reducing the resulting deflections. In addition, PZT has significantly larger dielectric constants than PVDF, thereby increasing the coupling between the charge equations and the momentum equations. Therefore, it becomes more important to model the electric potential.

Figures 3–8 contain the static deflection at the center of the plate for three different span ratios a/T and for all three of the previously mentioned theories. In Figures 3–5, the

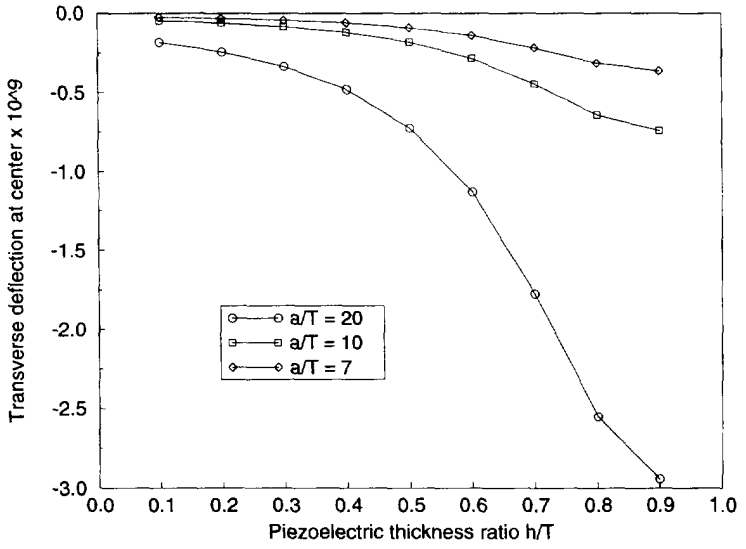

Fig. 2. Deflection *versus* piezoelectric thickness ratio for various theories (PVDF).

deflections are due to a unit potential uniformly applied to the top and bottom surfaces of the plate with the aluminium lamina being grounded. This corresponds to the same loading condition described for the laminates with PVDF. However, in this case modeling of the potential has some apparent effects, especially as the laminates become thicker and as the piezoelectric thickness ratios become larger. Note the percent differences indicated on the figures as well as the relative magnitudes of the deflections as the plates become thicker. Deflections in Figs 6–8 correspond to a unit voltage on a square patch at the center of the plate, with the side of the patch being one-third of the size of the plate. The remaining surfaces were grounded. In these cases the potential effects are more pronounced and are significant for thicker plates with high piezoelectric thickness ratios. It is interesting to note that for small piezoelectric thickness ratios, all three theories give nearly the same results. However, even for small piezoelectric thickness ratios ($h/T = 0.1$), the CPT theory begins to give slightly different results as the plates become thicker. This phenomenon does not appear to be related to modeling of the potential since the other two theories do not show

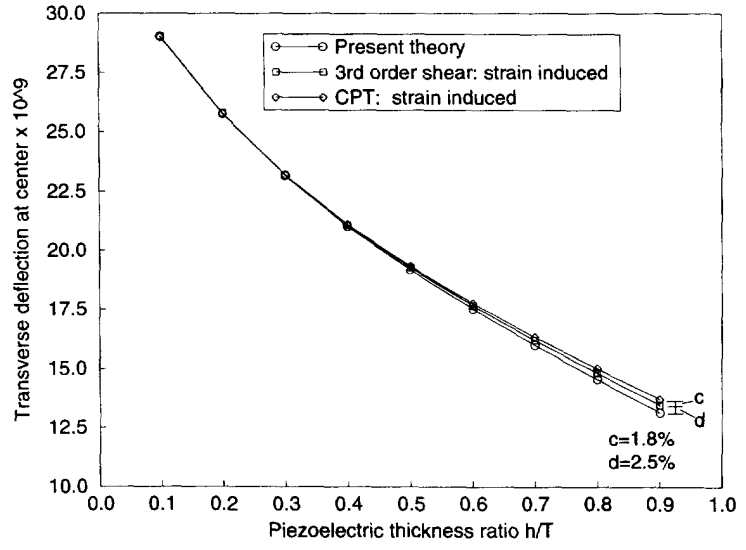

Fig. 3. Deflection *versus* piezoelectric thickness ratio (PZT: $a/T = 20$).

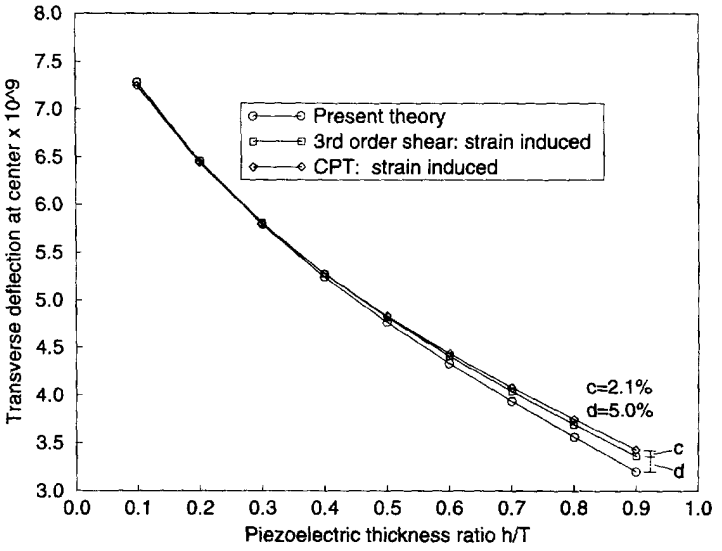

Fig. 4. Deflection *versus* piezoelectric thickness ratio (PZT: $a/T = 10$).

this; hence the effect must be related to the fact that shear deformation is not accounted for in the CPT.

Ignoring shear deformation seems to be the primary reason for differences in the calculated lowest natural frequencies given in Figs 9–11. Note that these frequencies have been non-dimensionalized according to $\bar{\omega} = \omega T\sqrt{\rho/c_{11}}$, where ω is the actual plate frequency, T is the plate thickness, and ρ and c_{11} are the mass density and material stiffness, respectively, for the aluminum. In the classical plate theory (CPT), shear deformation is not included and thus the plate is artificially stiffened, yielding a higher fundamental frequency. As the plate becomes thicker, this effect is pronounced, as expected. For high piezoelectric thickness ratios, the effect of modeling the potential is relatively the same for the three span ratios. Modeling the potential effectively stiffens the plate, thereby giving a

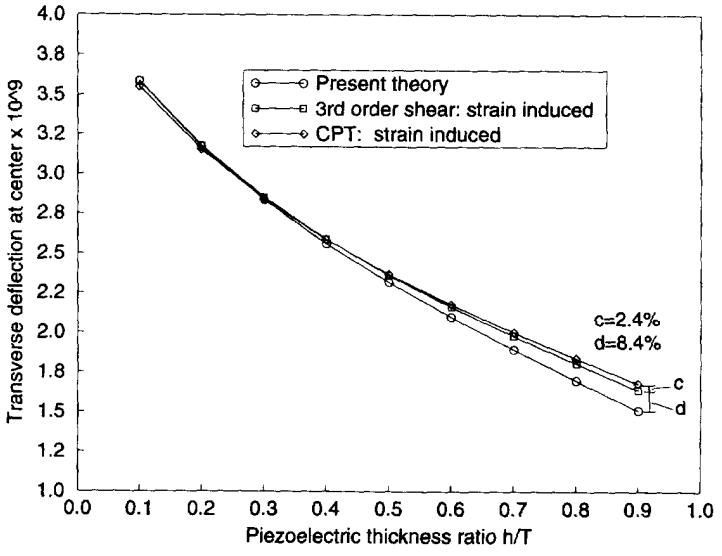

Fig. 5. Deflection *versus* piezoelectric thickness ratio (PZT: $a/T = 7$).

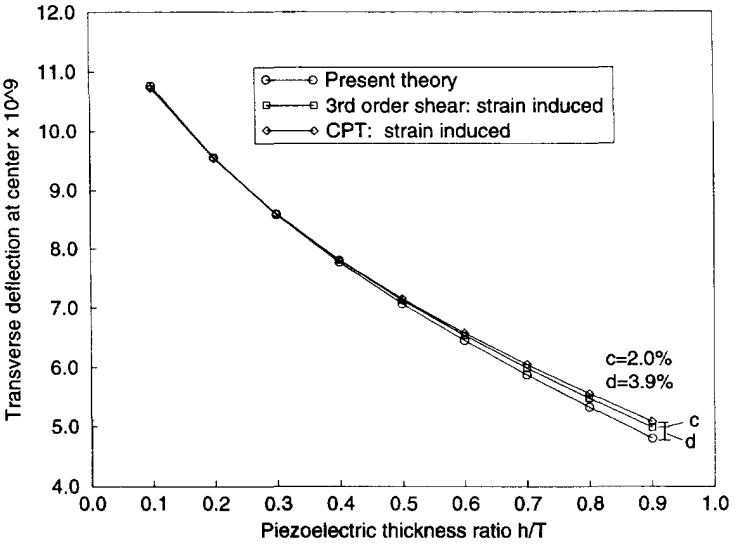

Fig. 6. Deflection *versus* piezoelectric thickness ratio (PZT : $a/T = 20$).

higher fundamental frequency, but this effect is largest when the piezoelectric thickness ratio is at its maximum.

5. CONCLUSIONS

In this paper, a hybrid theory for enhancing laminated plate theories to include piezoelectric laminae is presented. The theory is based on modeling the electric potential through the laminate thickness with 1-D finite elements. As a result of modeling the piezoelectric lamina, in-plane and out-of-plane displacement fields may become coupled for symmetric cross-ply laminates, and the nature and source of this coupling was briefly discussed. Simplifying assumptions concerning the charge equations were made so that

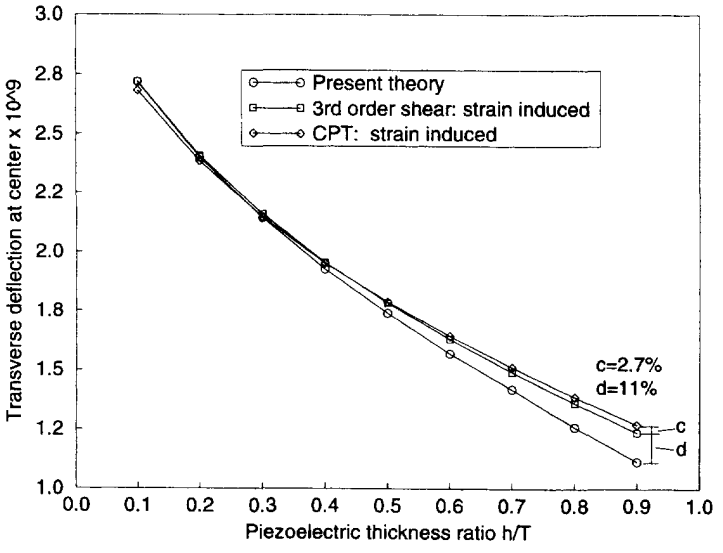

Fig. 7. Deflection *versus* piezoelectric thickness ratio (PZT : $a/T = 10$).

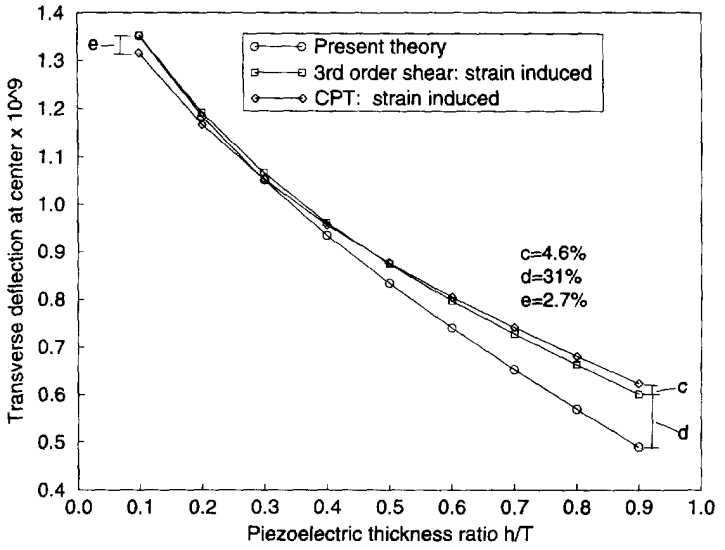

Fig. 8. Deflection *versus* piezoelectric thickness ratio (PZT: $a/T = 7$).

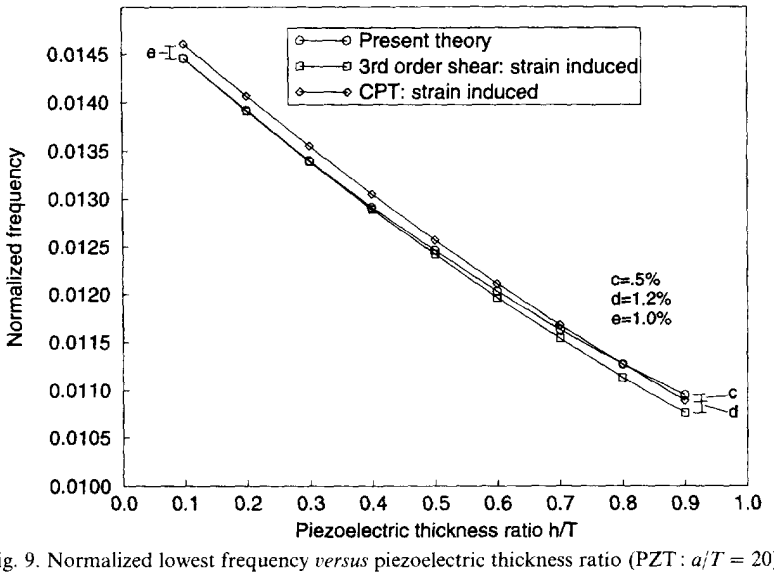

Fig. 9. Normalized lowest frequency *versus* piezoelectric thickness ratio (PZT: $a/T = 20$).

sensor equations could be derived, and these were compared with those from the literature. Finally, some numerical results were given for symmetric simply supported plates. Results indicate that thin piezoelectric laminae with a potential applied across the thickness direction can be modeled simply with strain induced methods. However, as the lamina becomes thicker, it becomes necessary to model the potential function, as is done here. For voltage loading conditions other than in the thickness direction, the model presented here is necessary, since the induced E field is not uniform.

Acknowledgements—The research reported in this paper is supported by Sandia National Laboratories, Albuquerque. The authors are grateful to Dr. Robert K. Thomas (Sandia) for the support.

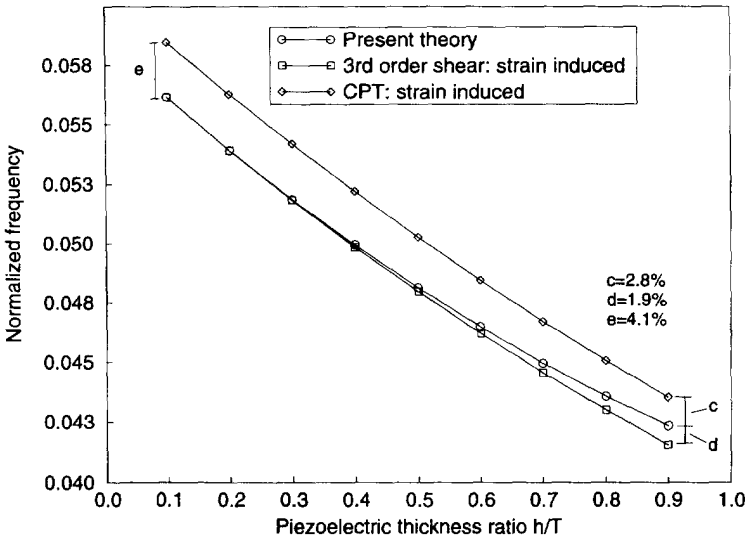

Fig. 10. Normalized lowest frequency *versus* piezoelectric thickness ratio (PZT: $a/T = 10$).

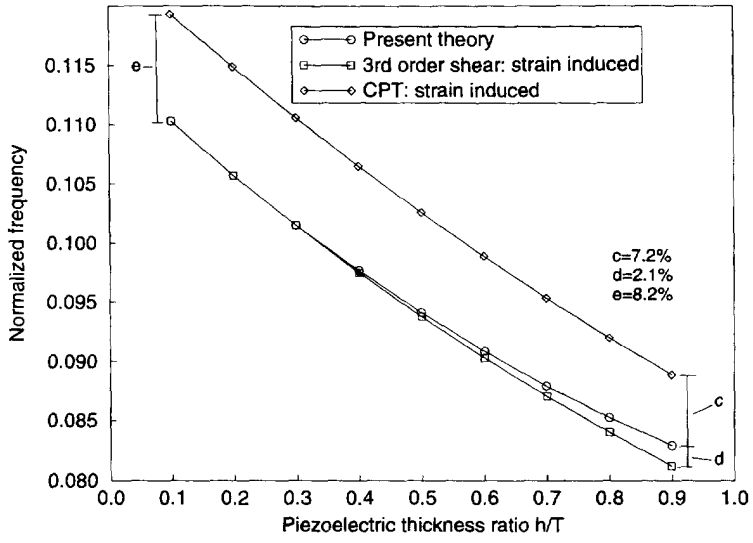

Fig. 11. Normalized lowest frequency *versus* piezoelectric thickness ratio (PZT: $a/T = 7$).

REFERENCES

Chandra, R. and Chopra, I. (1993). Structural modeling of composite beams with induced-strain actuators. *AIAA J.* **31**(9), 1692–1701.

Crawley, E. and de Luis, J. (1987). Use of piezoelectric actuators as elements of intelligent structures. *AIAA J.* **25**(10), 1373–1385.

Dunn, M. L. and Taya, M. (1993). Micromechanics predictions of the effective electroelastic moduli of piezoelectric composites. *Int. J. Solids Struct.* **30**(2), 161–175.

Hagood, N., Kindel, R., Ghandi, K. and Gaudenzi, P. (1993). Improving transverse actuation of piezoceramics using interdigitated surface electrodes. *Proc. SPIE, Smart Structures and Materials*, Albuquerque, New Mexico, 1993. Vol. 1917, Part One of two parts, pp. 341–352.

Im, S. and Atluri, S. N. (1989). Effects of a piezo-actuator on a finitely deformed beam subjected to general loading. *AIAA J.* **27**(12), 1801–1807.

Lee, C. K. (1990). Theory of laminated piezoelectric plates for the design of distributed sensors/actuators: part I: governing equations and reciprocal relationships. *J. Acoust. Soc. Am.* **87**(3), 1144–1158.

Lee, C. K. and Moon, F. C. (1990). Modal sensors and actuators. *J. Appl. Mech.* **57,** 434–441.
Nix, E. L. and Ward, I. M. (1986). The measurement of the shear piezoelectric coefficients of polyvinylidene flouride. *Ferroelectrics* **67,** 137–141.
Pai, P. F., Nayfeh, A. H., Oh, K. and Mook, D. T. (1993). A refined nonlinear model of composite plates with integrated piezoelectric actuators and sensors. *Int. J. Solids Struct.* **30**(12), 1603–1630.
Penfield, Jr., P. and Haus, H. A. (1967). *Electrodynamics of Moving Media.* MIT Press, Cambridge.
Reddy, J. N. (1984). A simple higher-order theory for laminated composite plates. *J. Appl. Mech.* **51,** 745–752.
Reddy, J. N. (1987). A generalization of two-dimensional theories of laminated composite plates. *Communications in Appl. Num. Meth.* **3,** 173–180.
Reddy, J. N. (1993). *An Introduction to the Finite Element Method,* 2nd edn. McGraw-Hill, New York.
Reddy, J. N. (1994). *Theory and Analysis of Laminated Composite Structures.* John Wiley & Sons, New York. In press.
Reddy, J. N. and Mitchell, J. A. (1994). Refined nonlinear theories of laminated composite structures with piezoelectric laminae. *Sadhana,* in press.
Tiersten, H. F. (1969). *Linear Piezoelectric Plate Vibrations.* Plenum, New York.
Tiersten, H. F. (1981). Electroelastic interactions and the piezoelectric equations. *J. Acoust. Soc. Am.* **70**(6).
Tzou, H. S. and Gadre, M. (1989). Theoretical analysis of a multi-layered thin shell coupled with piezoelectric shell actuators for distributed vibration controls. *J. Sound Vib.* **132**(3), 433–450.
Tzou, H. S. and Zhong, J. P. (1993). Electromechanics and vibrations of piezoelectric shell distributed systems. *J. Dynamic Systems, Measurement, and Control* **115,** 506–517.
Tzou, H. S., Zhong, J. P. and Natori, M. (1993). Sensor mechanics of distributed shell convolving sensors applied to flexible rings. *J. Vib. Acoustics* **115,** 40–46.
Varadan, V. V., Roh, Y. R., Varadan, V. K. and Tancrell, R. H. (1989). Measurement of all the elastic and dielectric constants of poled PVDF films. In 1989 *Ultrasonics Symposium,* pp. 727–730, IEEE, Montreal, Quebec, Canada.

APPENDIX

Mass inertia constants:

$$I_1 = \int_{-h/2}^{h/2} \rho \, dz, \quad I_3 = \int_{-h/2}^{h/2} \rho g_2(z) \, dz, \quad I_5 = \int_{-h/2}^{h/2} \rho g_1(z) g_2(z) \, dz,$$
$$I_2 = \int_{-h/2}^{h/2} \rho g_1 \, dz, \quad I_4 = \int_{-h/2}^{h/2} \rho g_1(z) g_1(z) \, dz, \quad I_6 = \int_{-h/2}^{h/2} \rho g_2(z) g_2(z) \, dz. \tag{A1}$$

Mechanical laminate stiffnesses:

$$A = \int_{-h/2}^{h/2} c \, dz, \quad \bar{A} = \int_{-h/2}^{h/2} g_1(z) c \, dz, \quad \bar{\bar{A}} = \int_{-h/2}^{h/2} g_2(z) c \, dz,$$
$$B = \int_{-h/2}^{h/2} g_1(z) g_1(z) c \, dz, \quad \bar{B} = \int_{-h/2}^{h/2} g_1(z) g_2(z) c \, dz,$$
$$D = \int_{-h/2}^{h/2} g_2(z) g_2(z) c \, dz, \quad F_{44} = \int_{-h/2}^{h/2} c_{44} \left(\frac{dg_1}{dz}\right)^2 dz,$$
$$F_{55} = \int_{-h/2}^{h/2} c_{55} \left(\frac{dg_1}{dz}\right)^2 dz, \tag{A2}$$

where

$$c = \begin{bmatrix} c_{11} & c_{12} & 0 \\ c_{12} & c_{22} & 0 \\ 0 & 0 & c_{66} \end{bmatrix}$$

Piezoelectric resultant constants

$$\beta_1^{jk} = \int_{z_{k-1}}^{z_k} \frac{df_j}{dz} dz, \quad \beta_2^{jk} = \int_{z_{k-1}}^{z_k} g_1(z) \frac{df_j}{dz} dz$$
$$\beta_3^{jk} = \int_{z_{k-1}}^{z_k} g_2(z) \frac{df_j}{dz} dz, \quad \alpha_4^{jk} = \int_{z_{k-1}}^{z_k} \frac{dg_1}{dz} f_j \, dz \tag{A3}$$

Material properties:

PZT:

$$C^{E} = \begin{bmatrix} 148 & 76.2 & 74.2 & 0 & 0 & 0 \\ & 148 & 74.2 & 0 & 0 & 0 \\ & & 131 & 0 & 0 & 0 \\ \text{symmetric} & & & 25.4 & 0 & 0 \\ & & & & 25.4 & 0 \\ & & & & & 35.9 \end{bmatrix} \text{GPa},$$

$$e^{T} = \begin{bmatrix} 0 & 0 & -2.1 \\ 0 & 0 & -2.1 \\ 0 & 0 & 9.5 \\ 0 & 9.2 & 0 \\ 9.2 & 0 & 0 \end{bmatrix} \frac{c}{m^2}, \quad \frac{k}{k_0} = \begin{bmatrix} 460 & 0 & 0 \\ 0 & 460 & 0 \\ 0 & 0 & 235 \end{bmatrix}, \tag{A4}$$

where e^{T} denotes traspose of matrix e, C^{E} denotes elastic stiffnesses at constant electric field, and

$$k_0 = 8.85 \times 10^{-12} \frac{c^2}{N - m^2}.$$

PVDF:

$$e^{T} = C^{E} d^{T} \tag{A5}$$

where

$$C^{E} = \begin{bmatrix} 3.61 & 1.61 & 1.42 & 0 & 0 & 0 \\ & 3.13 & 1.31 & 0 & 0 & 0 \\ & & 1.63 & 0 & 0 & 0 \\ & & & 0.55 & 0 & 0 \\ & & & & 0.59 & 0 \\ & & & & & 0.69 \end{bmatrix} \text{GPa},$$

$$d^{T} = \begin{bmatrix} 0 & 0 & 21.0 \\ 0 & 0 & 1.5 \\ 0 & 0 & -32.5 \\ 0 & -23 & 0 \\ -27 & 0 & 0 \\ 0 & 0 & 0 \end{bmatrix} \times 10^{-12} \frac{c}{N}, \quad \frac{k}{k_0} = \begin{bmatrix} 6.1 & 0 & 0 \\ 0 & 7.5 & 0 \\ 0 & 0 & 6.7 \end{bmatrix}.$$

Aluminum:

$$E = 70 \times 10^{9}\ \text{N m}^{-2}, \quad G = 26 \times 10^{9}\ \text{N m}^{-2}. \tag{A6}$$